International Journal of Pharmaceutics 529 (2017) 102–115

Contents lists available at ScienceDirect

International Journal of Pharmaceutics

journal homepage: www.elsevier.com/locate/ijpharm

Co-delivery of paclitaxel and anti-survivin siRNA via redox-sensitive oligopeptide liposomes for the synergistic treatment of breast cancer and metastasis

Xinyan Chen[a,c], Yidi Zhang[a], Chunming Tang[a], Chunli Tian[a], Qiong Sun[a], Zhigui Su[a], Lingjing Xue[a], Yifan Yin[a], Caoyun Ju[a,*], Can Zhang[a,b,*]

[a] State Key Laboratory of Natural Medicines, Jiangsu Key Laboratory of Drug Discovery for Metabolic Diseases, Center of Advanced Pharmaceuticals and Biomaterials, China Pharmaceutical University, Nanjing 210009, China
[b] State Key Laboratory of Pharmaceutical Biotechnology, Nanjing University, Nanjing 210046, China
[c] Pharmacy Faculty, Hubei University of Chinese Medicine, Wuhan 430065, China

ARTICLE INFO

Article history:
Received 24 March 2017
Received in revised form 15 June 2017
Accepted 18 June 2017
Available online 19 June 2017

Keywords:
Co-delivery
Paclitaxel
Anti-survivin siRNA
Redox-sensitive oligopeptide liposomes
Breast cancer
Synergistic inhibition

ABSTRACT

The overexpression of survivin in breast cancer cells is an important factor of paclitaxel (PTX) resistance in breast cancer. To overcome PTX resistance and improve the antitumor effect of PTX, we developed a novel liposome-based nanosystem (PTX/siRNA/SS-L), composed of a redox-sensitive cationic oligopeptide lipid ($LHSSG2C_{14}$) with a proton sponge effect, natural soybean phosphatidylcholine (SPC), and cholesterol for co-delivery of PTX and anti-survivin siRNA, which could specifically downregulate survivin overexpression. PTX/siRNA/SS-L exhibited high encapsulation efficiency and rapid redox-responsive release of both PTX and siRNA. Moreover, *in vitro* studies on the 4T1 breast cancer cells revealed that PTX/siRNA/SS-L offered significant advantages over other experimental groups, such as higher cellular uptake, successful endolysosomal escape, reduced survivin expression, the lowest cell viability and wound healing rate, as well as the highest apoptosis rate. In particular, *in vivo* evaluation of 4T1 tumor-bearing mice showed that PTX/siRNA/SS-L had lower toxicity and induced a synergistic inhibitory effect on tumor growth and pulmonary metastasis. Collectively, the collaboration of anti-survivin siRNA and PTX via redox-sensitive oligopeptide liposomes provides a promising strategy for the treatment of breast cancer and metastasis.

1. Introduction

Breast cancer remains a major threat to women's health around the world. In 2014, more than 200,000 women in the United States developed breast cancer and about 40,000 women died from this disease (Siegel et al., 2014). Although chemotherapy is commonly used in breast cancer treatment, it often causes drug resistance, which in turn restricts the efficacy of chemotherapy (Holohan et al., 2013). Gene therapy combined with chemotherapy has recently been considered as an alternative strategy to circumvent drug resistance that involves restoration of the sensitivity of cancer cells to chemotherapeutic drugs, thereby improving therapeutic efficacy (Lee et al., 2015; Li et al., 2016; Qu et al., 2014).

Paclitaxel (PTX), a microtubule stabilizing agent or mitotic inhibitor, is the first-line anticancer drug for the treatment of breast cancer (Jordan and Wilson, 2004). However, drug resistance in clinical practice is the maintain drawback for PTX application (Murray et al., 2012), which is associated with the upregulation of drug resistance proteins and mutations in the β-tubulin gene (Verma and Ramanathan, 2015). Recent studies have shown that PTX resistance is also related to the upregulation of anti-apoptotic proteins such as survivin, which is overexpressed in various breast cancer cells (Khan et al., 2014; Promkan et al., 2011; Wang et al., 2015). Notably, the expression level of survivin can be induced after PTX therapy (Ho et al., 2009; Hu et al., 2012), thereby resulting in

Abbreviations: ATCC, American Type Culture Collection; CLSM, confocal laser scanning microscopy; TEM, transmission electron microscopy; EE, entrapment efficiency; EPR, enhanced permeability and retention; GSH, glutathione; nS-L, non-reduction-sensitive blank liposome; PTX, Paclitaxel; SPC, soybean phosphatidylcholine; SS-L, reduction-sensitive blank liposome.

* Corresponding authors at: State Key Laboratory of Natural Medicines, Jiangsu Key Laboratory of Drug Discovery for Metabolic Diseases, Center of Advanced Pharmaceuticals and Biomaterials, China Pharmaceutical University, Nanjing 210009, China.
E-mail addresses: jucaoyun@cpu.edu.cn (C. Ju), zhangcan@cpu.edu.cn (C. Zhang)

http://dx.doi.org/10.1016/j.ijpharm.2017.06.071
0378-5173/

drug resistance (Singh et al., 2015), tumor recurrence (Jha et al., 2012), poor prognosis, low survival rate, and tumor metastasis (Chu et al., 2012; Parvani et al., 2015). Consequently, survivin gene knockout or downregulating survivin expression has become an attractive target for novel cancer treatment regimens (Coumar et al., 2013). Anti-survivin siRNA has emerged as a promising therapeutic agent due to its safety, tolerability, and the specificity of survivin gene silencing (Montazeri Aliabadi et al., 2011; Salzano et al., 2014, 2015). Therefore, the combination of PTX and anti-survivin siRNA might restore the sensitivity of breast tumor cells to PTX, thereby obtaining the synergistic anti-tumor effect and ultimately promoting patient compliance.

To accomplish the synergistic effect of PTX and anti-survivin siRNA on the treatment of breast cancer and metastasis, we constructed the redox-sensitive oligopeptide liposomes for co-delivering PTX and anti-survivin siRNA (PTX/siRNA/SS-L) based on a redox-sensitive cationic lipid (LHSSG2C$_{14}$), natural soybean phosphatidylcholine (SPC), and cholesterol, which would be more significant than sequentially delivering these in two separate carriers (Sun et al., 2011). Due to the different physiochemical properties of PTX and siRNA (Gandhi et al., 2014), PTX is encapsulated in the bilayer of the liposomes via hydrophobic effect, whereas siRNA is bound to the positively charged liposomes through electrostatic interaction (Fig. 1). The prepared redox-sensitive liposomes were expected to successfully escape endo-lysosomes via the proton sponge effect of histidine in LHSSG2C$_{14}$ after simultaneously delivering two drugs into the cells, and rapidly release two drugs through the breakdown of the disulfide bond in LHSSG2C$_{14}$, which is triggered by the reducing environment of the cytoplasm. The released anti-survivin siRNA can specifically downregulate survivin expression and increase PTX sensitization in the tumor cells, thereby resulting in the synergistic inhibition of growth and metastasis of breast cancer.

To prove the effectiveness of our design, the co-delivery liposomes were optimized by measuring the particle size, zeta potential, morphology, and encapsulated efficiency. Furthermore, the intracellular transport and the reductive-responsiveness of the co-delivery liposomes were evaluated. *In vitro* and *in vivo* antitumor efficacy studies were performed to assess the synergistic effect of co-delivery of survivin-targeted siRNA and PTX on the growth and metastasis of 4T1 murine breast cancer.

2. Materials and methods

2.1. Materials

Natural soybean phosphatidylcholine (SPC) was supported by Tai-Wei Pharmaceutical Co., Ltd. (Shanghai, China). Ditetradecyl 2-(4-(2-(2-(2-(2-(2,6-diaminohexanamido)-3-(1H-imidazol-4-yl) propanamido) ethyl) disulfanyl) ethylamino)-4-oxobutanamido) pentanedioate (LHSSG2C$_{14}$, Fig. A.1, Supplementary material) and ditetradecyl 2-(2-(2,6-diaminohexanamido)-3-(1H-imidazol-4-yl) propan-amido) pentanedioate (LHG2C$_{14}$, Fig. A.2, Supplementary material) as a control were synthesized by our group as previously described (Sun et al., 2015). Cholesterol and Nile red were obtained from Sigma-Aldrich (China). Paclitaxel was procured from

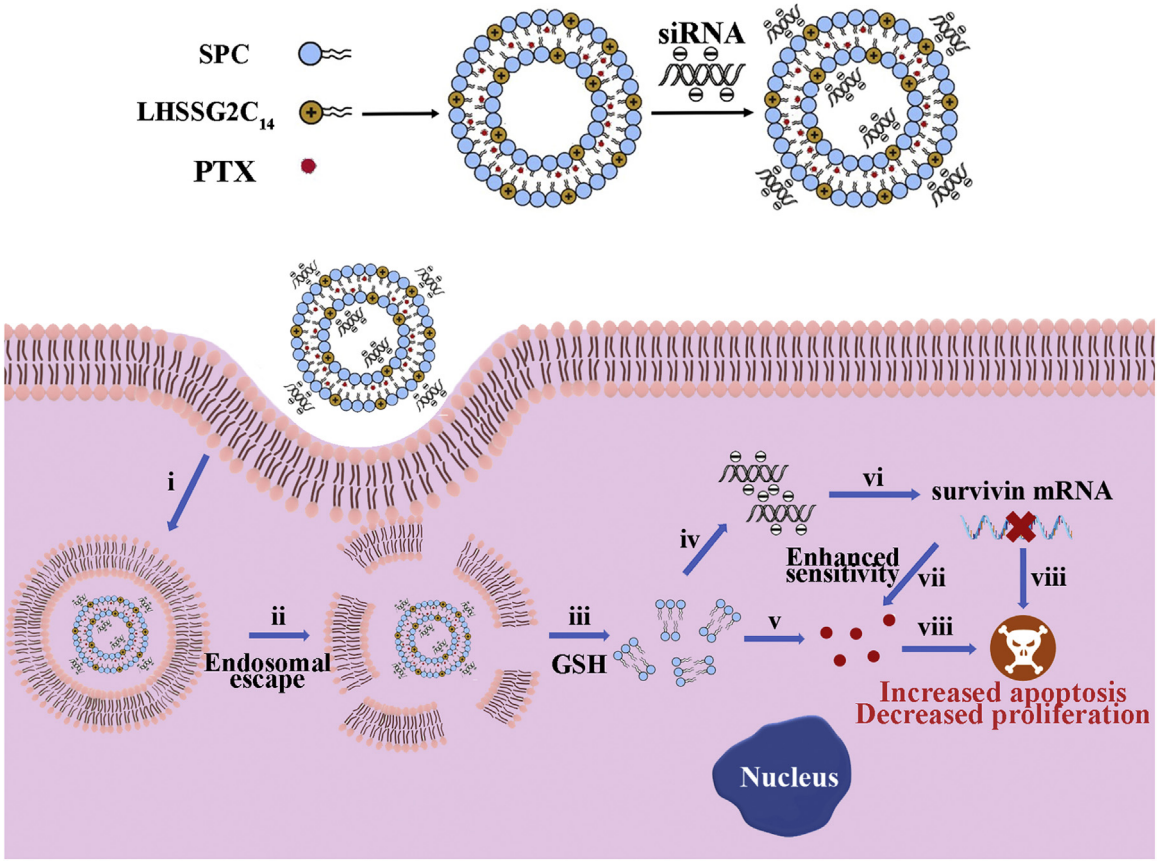

Fig. 1. Schematic illustration of the structure of redox-sensitive oligopeptide liposomes encapsulating PTX and siRNA, as well as the intracellular transport of the co-delivery system including endocytosis into endosomes (i), endosomal escape (ii), reduction-responsive liposomes disassembly (iii), siRNA release (iv), PTX release (v), downregulation of survivin mRNA expression (vi), enhanced sensitivity of tumor cells to PTX (vii), increased apoptosis and decreased proliferation induced by the combination of PTX and anti-survivin siRNA (viii).

Pureone Biotechnology (Shanghai, China). siRNA against survivin (CpusiRNA2, sense strand: 5′-GAAUUUGAGGAAACUGCGAtt-3′, anti-sense strand: 3′-ttCUUAAACUCCUUUGACGCU-5′), scrambled siRNA (siN.C.), as well as FAM-labeled siRNA (FAM-siRNA) were purchased from Biomics Biotechnologies Co., Ltd. (Nantong, China).

4T1 breast cancer cells were purchased from the American Type Culture Collection (ATCC) and cultured in RPMI 1640 medium containing 10% Gibco® FBS. The culture conditions included a temperature of 37 °C with a 5% CO_2 humidified atmosphere.

Female BALB/c mice, with ages of 6–8 weeks, were supplied by the Center for Disease Control and Prevention (Hubei, China). The mice were provided food and water in standard feeding condition, including an animal house with 12 h light and dark cycles. The Animal Ethics Committee of Hubei University of Chinese Medicine approved all animal experiments described in this study.

2.2. Methods

2.2.1. Preparation of PTX-loaded liposomes

The reduction-sensitive blank liposomes (SS-L) and non-reduction-sensitive blank liposomes (nS-L) as a control were prepared by using a film dispersion method as described elsewhere (Yang et al., 2014). First, SPC, cationic lipid (LHSSG2C_{14} or LHG2C_{14}), and cholesterol (5:5:1, w:w:w) were dissolved in a mixture of chloroform and methanol (1:1, v:v) in a pear-shaped bottle. After rotary evaporation at 40 °C and drying in a vacuum drier for 24 h to completely remove the organic solvent, the thin lipid membrane was hydrated with distilled water at 37 °C, and then sonicated for 10 min. Finally, the liposome solution was extruded using a 0.22 μm filter to remove the suspended solids. The PTX-loaded liposomes (PTX/SS-L and PTX/nS-L) were prepared by the same film dispersion method, simultaneously adding PTX to the organic solvent before the formation of the lipid film.

2.2.2. Preparation and characterization of PTX and siRNA co-loaded liposomes

PTX and siRNA co-loaded liposomes (PTX/siRNA/SS-L and PTX/siRNA/nS-L) were prepared by mixing siRNA and the PTX-loaded liposomes (PTX/SS-L or PTX/nS-L) at different N/P ratios (the molar ratio of the amine groups of the cationic lipid to the phosphate groups of siRNA). After standing for 30 min, 10 μL of the mixed solution was added to the pores of the 1% agarose gel to investigate whether siRNA was completely condensed by the PTX-loaded liposomes. siRNA staining was performed using GoldView™. The siRNA bands were visualized using a Gel DOC™ EZ Imager (Bio-Rad, USA) after electrophoresis for 15 min at 130 mV in 1 × TAE buffer.

2.2.3. Physicochemical properties of liposomes

The particle size, polydispersity index and zeta potential of liposomes were determined by dynamic light scattering (Nano ZS-90, Malvern, UK). Transmission electron microscopy (JEM1400, Japan) was used to assess the morphology of the liposomes after a drop of the liposome solution was placed on a carbon film and negatively stained with phosphotungstic acid.

2.2.4. PTX loading efficiency

The amount of PTX loaded into the liposomes was analyzed by HPLC (Dionex U3000, USA). The composition of the mobile phase, the flow rate, and the detection wavelength were as described by Ding et al. (2013). The entrapment efficiency (EE) of PTX was calculated as follows:

$$EE\% = \frac{\text{the amount of PTX loaded in liposome}}{\text{the amount of PTX fed totally}} \times 100\%$$

2.2.5. Glutathione-induced disassembly of blank liposomes

Glutathione-induced disassembly of SS-L was investigated by measuring the particle size, zeta potential and morphology after mixing 1 mL of the SS-L solution and 1 mL of 20 mM glutathione (GSH) at different time points. The nS-L incubated with 10 mM GSH was used as a control.

2.2.6. In vitro drug release

The release of PTX in response to different concentrations of GSH was performed according to the dialysis method described elsewhere (Jain et al., 2012). Briefly, the dialysis tube (MSCO 3500) containing 1 mL of the PTX/siRNA/SS-L solution was immersed in a release medium that consisted of 50 mL of 0.1 M PBS (pH 7.4), 1% Tween 80 (w/v), and different concentrations of GSH. During the experiment, the release medium was stirred using the magnetic stirrer at 100 rpm. At the specified time points, a 1-mL aliquot of the release medium was collected and replaced by 1 mL of fresh medium. The released amount of PTX was measured via high-performance liquid chromatography as earlier described. PTX release from PTX/siRNA/nS-L in response to 10 mM GSH was measured and used as a control. The release of siRNA from PTX/siRNA/SS-L (N/P = 5) in the presence of various concentrations of GSH was also monitored at specific time points by electrophoresis as earlier described.

2.2.7. Cellular uptake

Flow cytometry was employed to quantitatively compare the cellular uptake of siRNA packaged by liposomes and free siRNA. The redox-sensitive liposomes loaded with FAM-labeled siRNA (FAM-siRNA/SS-L and FAM-siRNA/PTX/SS-L) were prepared as earlier described for PTX/siRNA/SS-L. Approximately, 1×10^5 4T1 cells/mL were seeded onto each well of six-well plates containing RPMI 1640 culture medium supplemented with 10% fetal bovine serum. After 24 h, the cells were treated with free FAM-siRNA, FAM-siRNA/SS-L, and FAM-siRNA/PTX/SS-L for the prearranged time intervals (2, 4, 6 h), respectively. The concentration of FAM-siRNA in each well was fixed at 200 nM. The fluorescence intensity of FAM-siRNA was detected using the FACSCalibur system (BD Biosciences, USA). Meanwhile, cellular uptake of PTX was analyzed by HPLC. After 24 h of culture, the cells in the six-well plates were incubated with Taxol®, PTX/SS-L, and PTX/siRNA/SS-L for different time intervals (2, 4, 6 h), respectively. The concentration of PTX in each well was 50 μg/mL. The extraction method of PTX in cells was as previously described (Mo et al., 2011). The uptake amount of PTX was relative to the total protein content of cells.

2.2.8. Intracellular distribution and endosomal escape

To evaluate the intracellular distribution of co-delivery liposomes by confocal microscopy, PTX and siRNA were substituted for Nile red and FAM-siRNA, respectively. The preparation method for NR/FAM-siRNA/SS-L was similar to that of PTX/siRNA/SS-L. 4T1 breast cancer cells at a density of 1×10^4 cells/mL were cultured in a special glass dish for laser confocal detection and grew to about 40% confluence. After removing the original medium, the cells were treated with NR/FAM-siRNA/SS-L for 4 h. The concentrations of FAM-siRNA and Nile red in each well were 200 nM and 500 nM, respectively. Images of the cells were captured by confocal laser scanning microscopy (CLSM) (Olympus IX71, Japan) after staining with Hoechst 33245 at room temperature.

To establish the endosomal/lysosomal escape of co-delivery liposomes, the 4T1 cells were incubated with serum-free medium containing FAM-siRNA/PTX/SS-L for 2 h, and then the medium was replaced with a complete medium to continue the cultivation for 0 h and 2 h, respectively. After fixing with 4% paraformaldehyde and staining with LysoTracker™ Red, the cells were photographed by CLSM.

2.2.9. In vitro survivin expression level

The survivin mRNA and protein levels after treating the cells with different formulations were determined by quantitative real-time PCR and western blot analysis. After incubation in six-well plates for 24 h, the cells were treated with serum-free medium containing different formulations (SS-L/siNC, free siRNA, Taxol®, siRNA/SS-L, PTX/siNC/SS-L, PTX/siRNA/SS-L, and PTX/siRNA/nS-L) for 6 h. The final concentrations of siRNA (or siN.C.) and PTX in each well were 200 nM and 1.52 μM, respectively. Then, the cells were further cultured with complete medium for 24 h. The cellular total RNA and proteins in each well were respectively extracted using different reagents as described below.

For survivin mRNA analysis, total RNA was extracted using AZfresh™ RNA reagent (Azanno Biotech, Sweden), following the manufacturer's recommendations. The first cDNA was synthesized with 2 μg of RNA using BeyoRT™II cDNA (Beyotime Biotechnology, China). The reaction mixture containing the cDNA was then mixed with a ComSYBR qPCR Mix (Novland Biopharma, China) and the primers of the survivin gene (forward 5′-AGCATAGAAAG-CACTCCCCT-3′ and reverse 5′-CAATTGACTGACGGGTAGTC-3′) or GAPDH gene (forward 5′-TTCACCACCATGGAGAAGGC-3′ and reverse 5′-GGCATGGACTGTGGTCATGA-3′) as internal reference and subjected to 40 PCR amplification cycles of 94 °C for 15 s, 63 °C for 40 s, and 70 °C for 90 s. Quantification of cDNA was performed using a CFX96™ real-time system (Bio-Rad, USA). All of the quantitative reverse transcription-PCR experiments were performed in triplicate.

In the survivin protein assay, 80 μL of a lysis buffer (Beyotime Biotechnology, China) containing 1 mM of PMSF was added to each well of the six-well plates and then placed on ice for 30 min. After the determination of protein concentration by using an xMark™ spectrophotometer (Bio-Rad, USA) at a wavelength of 562 nm, 20 μg of the total proteins was denatured, separated on 15% PAGE-SDS gels, and then transferred onto PVDF membranes by using a Trans-Blot Turbo (Bio-Rad, USA). Subsequently, the proteins on the membranes were blocked and incubated with survivin antibodies (Abcam, 1:1000) and HRP-labeled goat anti-rabbit IgG (Beyotime, 1:1000), and then detected using BeyoECL Plus.

2.2.10. Cell viability assay

The cytotoxicity effect of PTX and anti-survivin siRNA was assessed by the MTT assay. After adherent growth on 96-well plates, the 4T1 cells were treated with SS-L/siNC, free siRNA, Taxol®, siRNA/SS-L, PTX/siNC/SS-L, PTX/siRNA/SS-L, and PTX/siRNA/nS-L for 24 h, respectively. The concentration of PTX was changed from 0.22 μg/mL to 1.32 μg/mL. The absorbance of each well was detected by using an xMark™ spectrophotometer at a wavelength of 570 nm.

2.2.11. Wound healing test

The wound healing test was performed to explore the migration impact of siRNA/SS-L on the tumor cells. When the adherent cells in the six-well plates reached 80% confluence, scratch wounds were made in each well by using a 10-μL sterilized tip, and the cells were washed with PBS thrice to remove the floating cells. Then, 1.8 mL of the serum-free medium and 0.2 mL of the free siRNA or siRNA/SS-L solution were added into each well, respectively. Untreated cells were used as a control. The concentration of siRNA per well was 50 nM. The wounds were observed on an inverted microscope (Olympus CKX31, Japan). The wound healing rate was analyzed by comparing the width of the wounds before and after drug treatment.

2.2.12. Cell apoptosis assay

The procedures for cell culture and drug treatment in the cell apoptosis assay were similar to that of *in vitro* survivin expression analysis. The trypsinization, collection, and resuspension of the 4T1 cells in binding buffer were as described in the Annexin V-FITC/PI apoptosis detection kit (Beyotime Biotechnology, China). The fluorescence intensity of the stained cells was determined by flow cytometry.

2.2.13. In vivo pharmacodynamics study

Approximately 0.2 mL of the cell suspension at a density of 1×10^6 cells/mL was injected into the right armpits of female BALB/c mice after one week of acclimatization. When the tumors grew to about 150 mm^3, the mice were randomly distributed into five groups (n = 5) and respectively administered with PBS, siRNA/SS-L, PTX/siNC/SS-L, PTX/siRNA/SS-L, and PTX/siRNA/nS-L by tail vein injection at a PTX dose of 1 mg/kg and siRNA dose of 1.5 mg/kg for 5 times every three days. The length (L) and width (W) of tumors and the body weight of the mice were measured before each injection. Tumor volume (V) was calculated using the following formula: $V = (L \times W^2)/2$. At the 15th day after the first injection, the mice were sacrificed, and tissues of the tumor, lungs, and other organs (heart, spleen, kidney and liver) were collected. After cleaning with PBS and drying with filter paper, the tissues were weighed. Subsequently, the tumor tissues were randomly selected from each group and halved; one portion was fixed in formalin and then stained with H & E for histological evaluation of antitumor ability, and the other was used in the analysis of survivin expression level *in vivo*. Meanwhile, the lung tissues and other organs were also fixed and stained to assess for pulmonary metastasis and other toxic effects.

2.2.14. Statistical analysis

Data were expressed as the mean ± SD and statistically analyzed using the student's *t*-test. Statistical differences between two groups were considered at $p < 0.05$, and statistical significance was considered at $p < 0.01$ or $p < 0.001$.

3. Results and discussion

3.1. Preparation and characterization of liposomes

The blank liposomes (SS-L and nS-L) were prepared by using the film dispersion method, and the weight ratio of $LHSSG2C_{14}$ and SPC was screened to gain smaller and uniform particle size (Table A.1, Supplementary material). Under the optimal weight ratio of 1:1, SS-L displayed a smaller and uniform particle size of 76.7 ± 2.4 nm with a polydispersity index of 0.178 ± 0.021, and a positive zeta potential of +25.5 ± 1.8 mV (Table 1).

The redox-sensitive oligopeptide liposomes loading PTX (PTX/SS-L) were prepared by the same film dispersion method. The weight ratio of PTX to total lipids (the sum of $LHSSG2C_{14}$ and SPC) was also screened to obtain high entrapment efficiency of PTX. PTX/SS-L exhibited the highest entrapment efficiency [95.8 ± 2.8% (w/w)] and the smallest particle size (92.3 ± 1.6 nm) when the weight ratio of PTX to total lipids was 1:60 (Table 1). In the control, non-sensitive oligopeptide liposomes loading PTX (PTX/nS-L) were prepared at the same weight ratio of 1:60, which had a similar entrapment efficiency (93.6 ± 3.2%) and zeta potential (+21.6 ± 2.5 mV), but a slightly larger particle size (110.5 ± 1.5 nm) than that of PTX/SS-L.

After the successful encapsulation of PTX, the siRNA loading ratio (N/P ratio) was surveyed by measuring the particle size and zeta potential of PTX/siRNA/SS-L (Fig. 2a). The zeta potential of PTX/siRNA/SS-L changed from ~−12.3 mV to ~25.8 mV, with an increase in N/P ratio from 0.5 to 8. Meanwhile, particle size significantly decreased from ~537 nm to nearly 150 nm and showed minimal to negligible change when the N/P ratio reached ~5, which indicated that PTX/siRNA/SS-L had formed a compact

Table 1
The characteristic parameters of liposomes.

Liposomes	Weight ratio [a]	Particle size (nm)	Polydispersity index	Zeta potential (mV)	EE (%)
SS-L	/	76.7 ± 2.4	0.178 ± 0.021	+25.5 ± 1.8	/
nS-L	/	89.1 ± 3.1	0.158 ± 0.034	+24.1 ± 1.7	/
PTX/SS-L	1:20	198.5 ± 3.1	0.320 ± 0.014	+23.9 ± 2.3	32.7 ± 3.6
PTX/SS-L	1:40	145.4 ± 3.7	0.236 ± 0.016	+21.8 ± 2.6	79.2 ± 3.4
PTX/SS-L	1:60	92.3 ± 1.6	0.236 ± 0.017	+23.4 ± 2.7	95.8 ± 2.8
PTX/nS-L	1:60	110.5 ± 1.5	0.271 ± 0.013	+21.6 ± 2.5	93.6 ± 3.2
PTX/siRNA/SS-L	1:60	156.4 ± 2.1	0.156 ± 0.012	+15.2 ± 1.4	95.8 ± 2.8
PTX/siRNA/nS-L	1:60	178.5 ± 2.6	0.189 ± 0.015	+16.4 ± 2.1	93.6 ± 3.2

[a] Weight ratio of PTX to total lipids (the sum of LHSSG2C$_{14}$ and SPC).

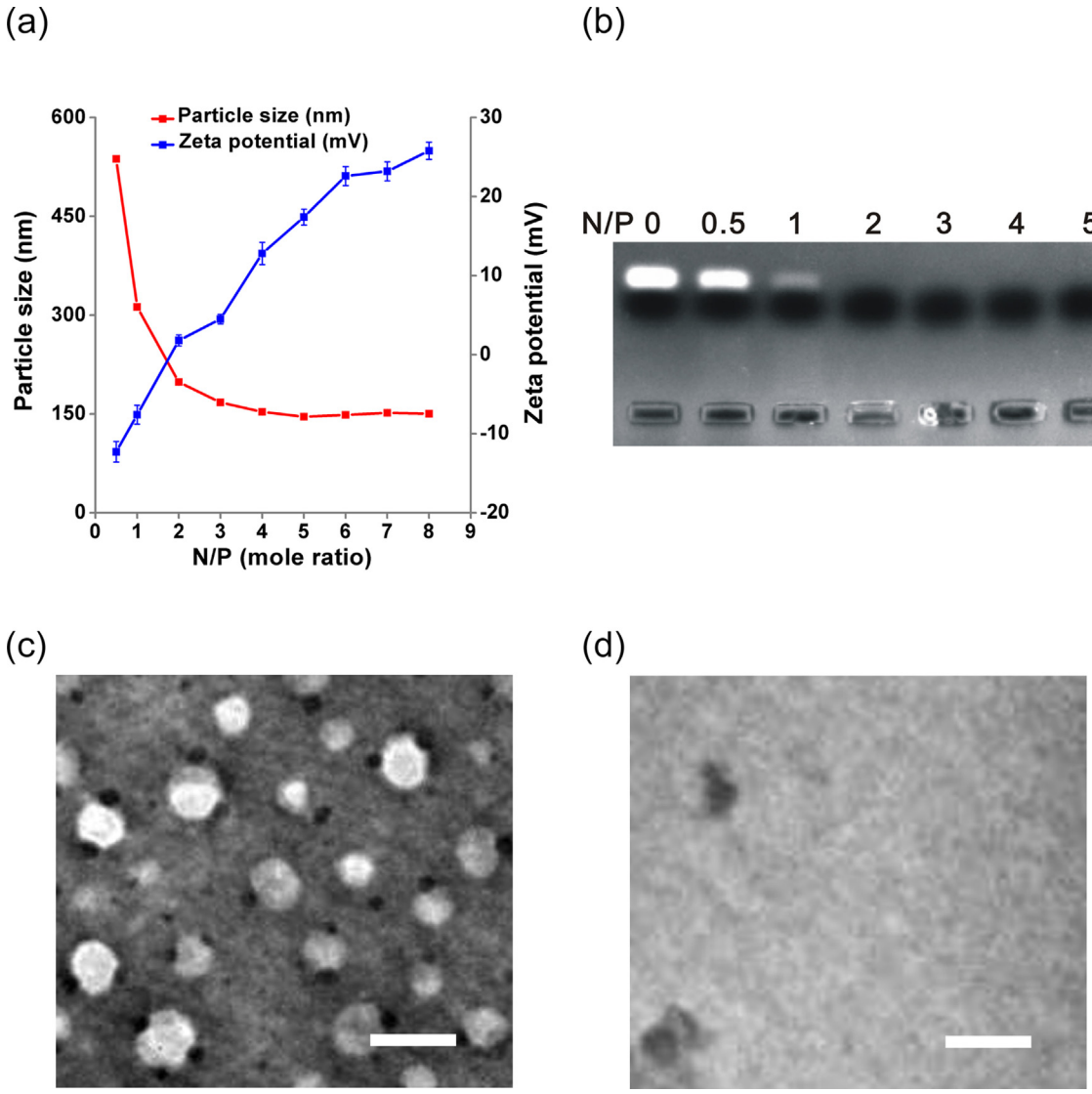

Fig. 2. (a) Particle size and zeta potential of PTX/siRNA/SS-L at different N/P ratios. (b) Agarose gel electrophoresis assay of PTX/siRNA/SS-L at different N/P ratios. (c) TEM image of PTX/siRNA/SS-L, Scale bar: 200 nm. (d) TEM image of SS-L after incubation with 10 mM GSH for 24 h, Scale bar: 100 nm.

structure at an N/P ratio of 5. Furthermore, agarose gel electrophoresis was conducted to determine whether stable PTX/siRNA/SS-L was formed with no leakage of siRNA. As shown in Fig. 2b, the siRNA band disappeared at an N/P ratio greater than 2, indicating a complete formation of PTX/siRNA/SS-L. Based on these findings, the optimal N/P ratio of 5 was used in the preparation of PTX/siRNA/SS-L in the subsequent experiments. The particle size, zeta potential, and polydispersity index of PTX/siRNA/SS-L at an N/P ratio of 5 were 156.4 ± 2.1 nm, +15.2 ± 1.4 mV, and 0.156 ± 0.012, respectively. The spherical morphology of PTX/siRNA/SS-L at an N/P ratio of 5 was observed by TEM (Fig. 2c), which further validated that the redox-sensitive oligopeptide liposomes with highly efficient encapsulation of PTX and siRNA were successfully prepared. PTX/siRNA/SS-L with a particle size of

less than 200 nm might take advantage of the enhanced permeability and retention (EPR) effect to passively target tumors (Kobayashi et al., 2014).

3.2. GSH-triggered disassembly of blank liposomes

To evaluate the sensitivity of disulfide bond in LHSSG2C_{14} to the redox environment in the cytoplasm, we measured the particle size and zeta potential of SS-L incubated with 10 mM GSH simulating the intracellular environment (Li et al., 2012) for different time intervals. The result was shown in Fig. 3a, with increasing incubation time from 0 h to 8 h, the particle size of SS-L significantly increased from ~76.7 nm to ~890.1 nm, and the zeta potential changed from ~15.1 mV to ~−17.7 mV accordingly, which were indicative of the disassembly of SS-L in the presence of 10 mM GSH, which was also confirmed by the disappearance of the spherical morphology of SS-L in the TEM images after incubation with 10 mM GSH for 24 h (Fig. 2d). By comparison, the particle size and zeta potential of nS-L without the GSH-sensitive disulfide bond did not significantly change, even after incubation with 10 mM GSH for a longer time (Fig. A.3, Supplementary material). These results explained that the destruction of SS-L was derived from the cleavage of the disulfide bond in LHSSG2C_{14} that was triggered by 10 mM GSH. The reduction-responsive disassembly of SS-L would be beneficial for the rapid release of co-loaded drugs from the redox-sensitive liposomes in the cytoplasm.

3.3. In vitro release of PTX and siRNA

Fig. 3b shows the release of PTX from PTX/siRNA/SS-L in response to different concentrations of GSH. As expected, the release of PTX from PTX/siRNA/SS-L was relatively slow at a GSH concentration of 10 μM, which simulated the extracellular environment, and the accumulated release of PTX was only about 8% for the first 4 h and less than 30% for 36 h, implying that PTX/siRNA/SS-L was relatively stable under the physiological environment. The release of PTX from PTX/siRNA/SS-L was much faster in a cytoplasmic environment with a GSH concentration of 10 mM, and the accumulated release of PTX was close to 50% for the first 4 h and more than 80% for 36 h. Moreover, PTX/siRNA/nS-L as a control only released less than 25% of PTX after incubation with 10 mM GSH for 36 h. Consequently, it was suggested that the cleavage of the disulfide linkage in LHSSG2C_{14} contributed to the rapid release of PTX.

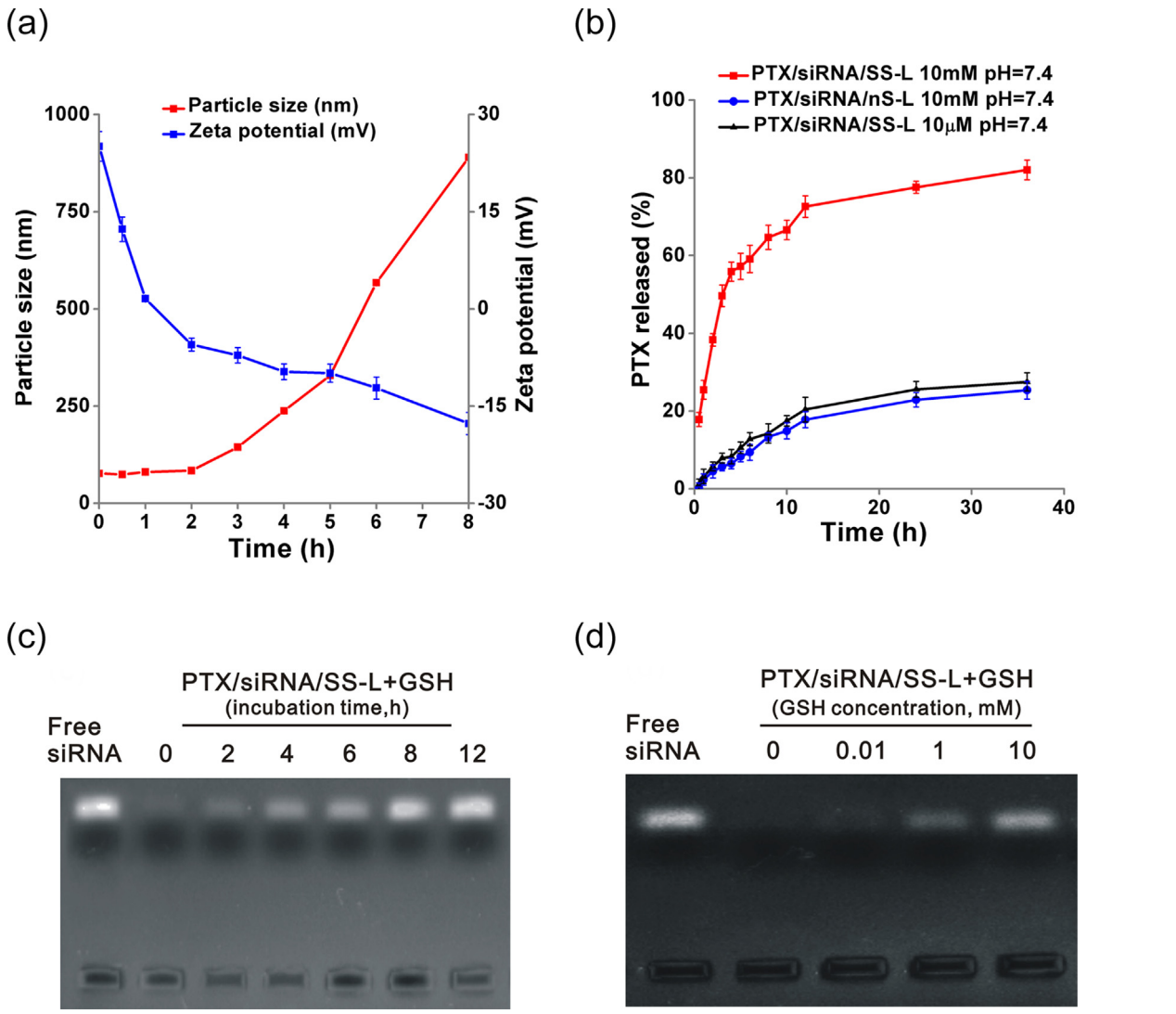

Fig. 3. (a) Particle size and zeta potential of SS-L in the presence of 10 mM GSH for different time intervals. (b) PTX release from PTX/siRNA/SS-L and PTX/siRNA/nS-L after treating with different concentrations of GSH for different time points. (c) Agarose electrophoresis assay of the siRNA release from PTX/siRNA/SS-L after treating with 10 mM GSH for different time points. (d) Agarose electrophoresis assay of the siRNA release from PTX/siRNA/SS-L after treating with different concentrates of GSH for 8 h.

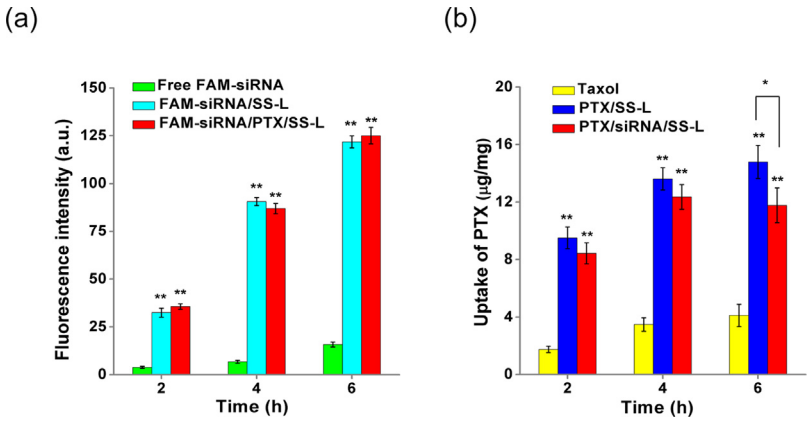

Fig. 4. Cellular uptake of FAM-siRNA (a) and PTX (b) at different time points. Free FAM-siRNA and Taxol® as control groups, $^{*}p < 0.05$, $^{**}p < 0.01$.

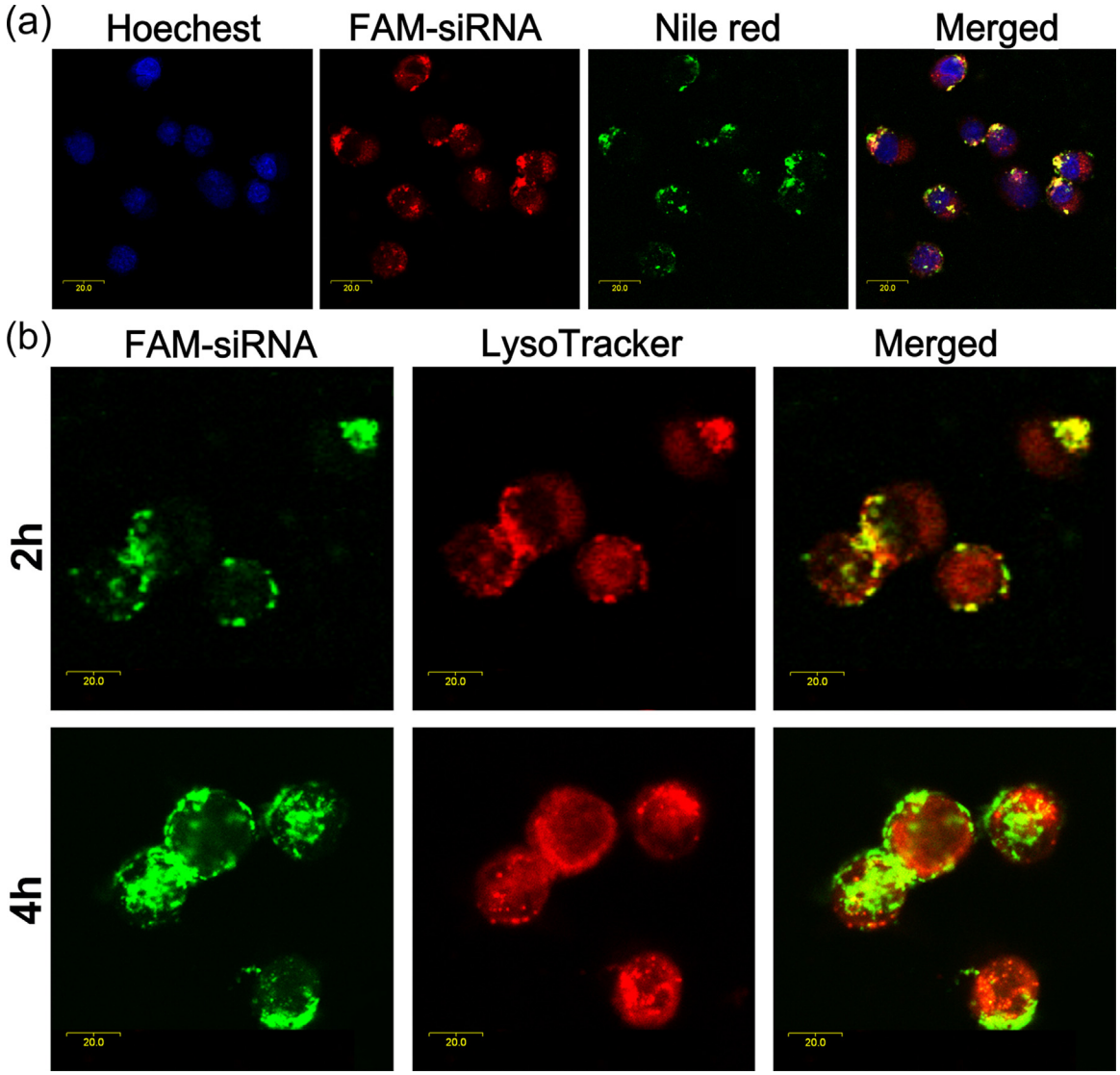

Fig. 5. Intracellular distribution of NR/FAM-siRNA/SS-L (a) and intracellular transport of FAM-siRNA/PTX/SS-L (b) after treatment for 2 h and 4 h, respectively. Scale bar: 20.0 μm.

The release of siRNA was also observed in the agarose electrophoresis experiment. The bands of siRNA were clearly detected after 2 h of incubation with 10 mM GSH (Fig. 3c), but were not observed even after incubation with 10 μM GSH for 8 h (Fig. 3d), indicating that siRNA was rapidly released in the presence of a high concentration of GSH in the cytoplasm, whereas minimal to negligible siRNA was released in an extracellular environment with a low GSH concentration. The results of *in vitro* drug release study showed that PTX/siRNA/SS-L is a stable co-delivery system during blood circulation with no leakage of payloads, yet rapidly releases the drugs once into the cytoplasm, thus fully exerting the anti-tumor efficacy of PTX and siRNA.

3.4. Cellular uptake

To evaluate the ability of the redox-sensitive oligopeptide liposomes to improve cellular uptake of drugs, we quantitatively measured the intracellular concentration of FAM-siRNA and PTX by using different methods. Fig. 4a and b shows that the cellular uptake of FAM-siRNA and PTX were both time-dependent, and the uptake amount increased with the prolongation of incubation time. After 2 h of incubation time, PTX/siRNA/SS-L and FAM-siRNA/PTX/SS-L exhibited 3.9-fold and 6.7-fold higher cellular uptake than Taxol® and free FAM-siRNA, respectively ($p < 0.01$), which indicated that the redox-sensitive oligopeptide liposomes could

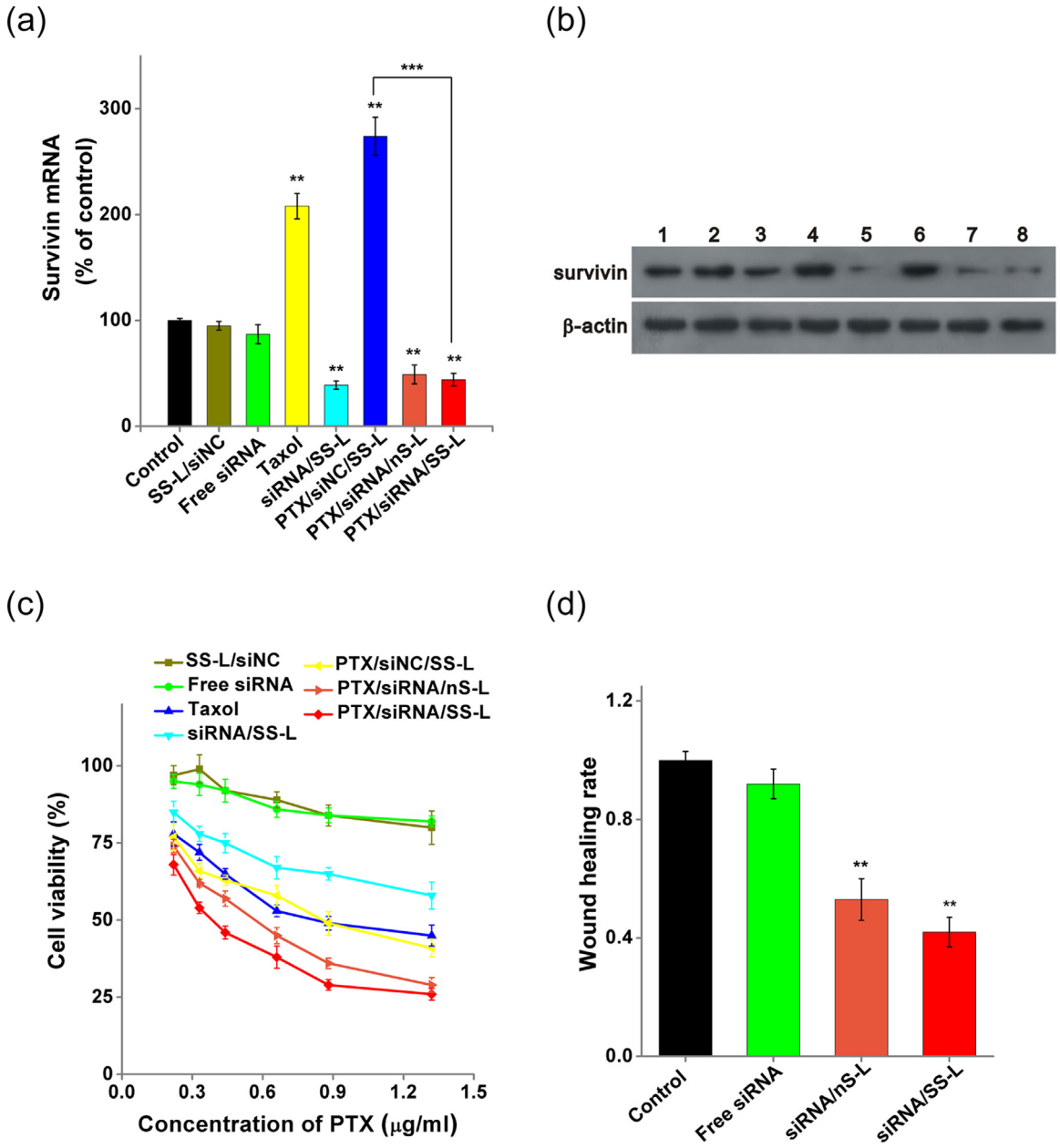

Fig. 6. *In vitro* studies of PTX/siRNA/SS-L on 4T1 breast tumor cells. (a) The expression of survivin mRNA in the 4T1 cells after incubation with different formulations compared to that in the control group. (b) Survivin protein expression determined by western blot analysis. 1: control; 2: SS-L/siNC; 3: Free siRNA; 4: Taxol®; 5: siRNA/SS-L; 6: PTX/siNC/SS-L; 7: PTX/siRNA/nS-L; 8: PTX/siRNA/SS-L. (c) Cell viability assay after treating with different formulations for 24 h. PTX concentrations ranged from 0.22 μg/mL to 1.32 μg/mL. (d) The wound healing rate of 4T1 cells incubated with different formulations for 24 h. $^{*}p < 0.05$, $^{**}p < 0.01$, $^{***}p < 0.001$.

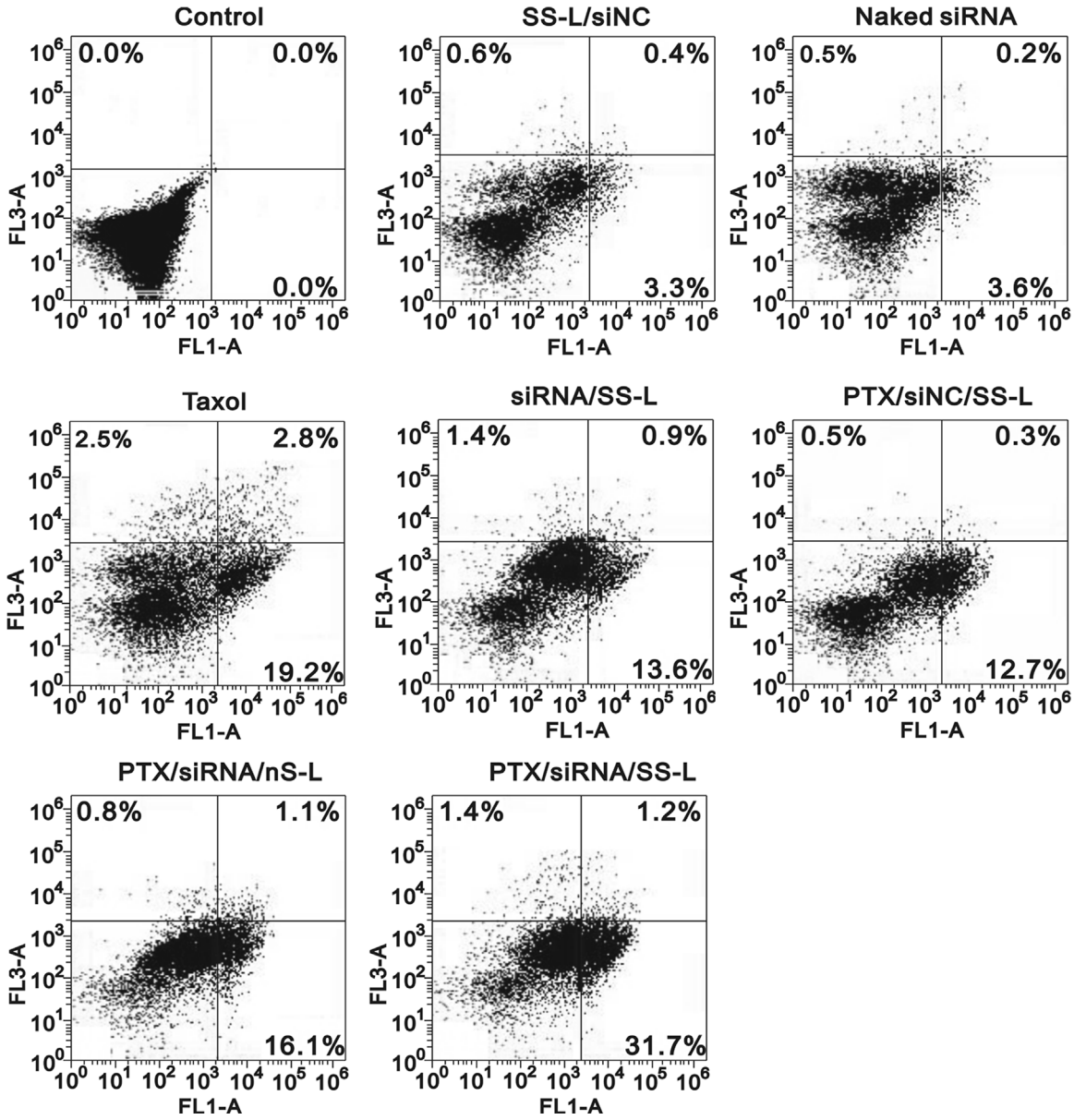

Fig. 7. Cell apoptosis of 4T1 cells after treatment with different formulations by the Annexin V-FITC/PI assay.

effectively facilitate drug delivery into tumor cells. In addition, FAM-siRNA/SS-L and FAM-siRNA/PTX/SS-L showed similar cellular uptake of FAM-siRNA at different time points, implying that small difference in particle size between FAM-siRNA/SS-L and FAM-siRNA/PTX/SS-L did not impact the cellular uptake of FAM-siRNA. However, the PTX uptake of PTX/SS-L was significantly higher than that of PTX/siRNA/SS-L, especially at the uptake time of 6 h ($p < 0.05$). This result could be explained by the fact that PTX/SS-L had stronger positive electricity compared with PTX/siRNA/SS-L, thus favoring adhesion of the negatively charged cytomembrane (Fröhlich, 2012). Hence, to eliminate the potential difference between PTX/SS-L and PTX/siRNA/SS-L, non-therapeutic siRNA (scrambled siRNA) was applied to incorporate into SS-L and PTX/SS-L in the following experiments.

3.5. Intracellular distribution and endosomal escape

Nile red is a lipophilic triphenodioxazine fluorescent dye that is often used to replace PTX in laser confocal microscopy studies (Yang et al., 2014). Therefore, FAM-siRNA and Nile red were selected and used as replacements for siRNA and PTX to determine the subcellular distribution of co-delivery liposomes in the 4T1 cells. After incubation with NR/FAM-siRNA/SS-L for 4 h, a remarkable yellow area representing the co-localization of red fluorescence (Nile red) and green fluorescence (FAM-siRNA) was observed around the blue-stained nuclei by CLSM (Fig. 5a), indicating that the redox-sensitive oligopeptide liposomes simultaneously delivered PTX and siRNA into the cells, and thus could impart a synergistic anti-tumor effect.

To avoid the degradation of siRNA and PTX by large amounts of enzymes and the acidic environment of endolysosomes, the redox-sensitive oligopeptide liposomes were expected to show an ability to escape endolysosomal engulfment and subsequent degradation. According to our previous report (Sun et al., 2015), liposomes made of a cationic oligopeptide lipid ($LHSSG2C_{14}$) can potentially escape from the endolysosomes due to the proton sponge effect of its cationic head of lysine and histidine (Midoux et al., 2009; Mo et al., 2012). Therefore, the co-delivery liposomes comprising the same

LHSSG2C$_{14}$ should have a similar ability of endolysosomal escape. To confirm this hypothesis, the intracellular transport of FAM-siRNA/PTX/SS-L was observed by CLSM. As shown in Fig. 5b, after incubation for 2 h, the green fluorescence of FAM-siRNA overlapped with the red fluorescence of LysoTracker™, proving that FAM-siRNA/PTX/SS-L was effectively taken up by the 4T1 cells and then entrapped in the endolysosomes. However, the green fluorescence was obviously separated from the red fluorescence after an additional 2 h of incubation, suggesting that FAM-siRNA/PTX/SS-L could successfully escape from the endolysosomes and move into the cytoplasm. This escape may involve the histidine in the cationic head of LHSSG2C$_{14}$, which can extensively absorb protons and enhance the osmotic pressure in the endolysosomes, thereby causing the disruption of endolysosomes (Shigeta et al., 2007).

3.6. In vitro survivin expression level

Ling et al. (2004) have reported that the expression of survivin in breast cancer cells is rapidly upregulated by PTX within 6 h, which results in cellular resistance to PTX and subsequently weakens the ability of PTX to kill tumor cells. To verify that co-delivery of anti-survivin siRNA and PTX can inhibit the PTX-induced upregulation of survivin expression, intracellular survivin levels were quantified after transfection with different formulations. Compared with the control group, Taxol® and PTX/siNC/SS-L markedly elevated the expression of survivin mRNA in the 4T1 cells ($p < 0.01$, Fig. 6a). Furthermore, the expression of survivin in the 4T1 cells treated with PTX/siNC/SS-L was upregulated to 282% of that of the control group, which was significantly higher than that of the Taxol® group at the same PTX concentration, which was probably due to the higher cellular uptake of PTX after encapsulation by redox-sensitive oligopeptide liposomes. In contrast, the cells treated with PTX/siRNA/SS-L exhibited a 57% downregulation of survivin mRNA expression compared with the control group ($p < 0.01$), which was higher than the 51% decrease in PTX/siRNA/nS-L, thereby validating that the addition of siRNA against survivin inhibited the PTX-induced upregulation of survivin expression, and the rapid intracellular release of siRNA from redox-sensitive oligopeptide liposomes in the cytoplasm led to the enhancement of survivin-silencing efficiency. These findings were also supported by the results of western blot analysis, which indicated the expression of survivin protein in the 4T1 cells (Fig. 6b).

3.7. Cell viability assay

The anti-proliferative effects of co-delivery liposomes and mono-delivery liposomes, as well as free drugs on the 4T1 cells were assessed by the MTT assay. Fig. 6c shows that after treatment with SS-L/siNC for 24 h, more than 80% of the cells were alive at the concentration range of PTX, indicating that the redox-sensitive liposomal nanocarrier assembled by LHSSG2C$_{14}$ and SPC is a relatively safe drug delivery carrier. Compared with the siRNA/SS-L group, the free siRNA group exhibited a lower cytotoxicity due to the lower cellular uptake of siRNA. However, the Taxol® group and PTX/siNC/SS-L showed similar degrees of cytotoxicity, probably due to the toxicity of Cremophor EL as the solubilizer of PTX. Notably, PTX/siRNA/SS-L showed the strongest inhibitory effect on the 4T1 breast cancer cells, with an IC$_{50}$ value of 0.35 μg/mL, which was lower than that of PTX/siNC/SS-L (0.82 μg/mL) and the Taxol® group (0.85 μg/mL), thereby reflecting that the addition of anti-survivin siRNA, as well as the involvement of redox-sensitive oligopeptide liposomes improved the anti-proliferative effect of PTX on the 4T1 breast cancer cells. We thus inferred that the enhanced ability of PTX in killing tumor cells was attributable to the downregulation of survivin expression by anti-survivin siRNA, which recovered the sensitivity of the 4T1 breast cancer cells to PTX.

3.8. Wound healing test

One major hurdle in the clinical treatment of breast cancer is metastasis and the occurrence of a secondary tumor (Marino et al., 2013), which are associated with the upregulation of survivin expression. A wound healing experiment was conducted to study the effect of downregulating survivin expression on the migration of 4T1 breast cancer. Considering the cytotoxicity of PTX, the 4T1 cells were incubated with siRNA/SS-L. The wound healing rate was shown in Fig. 6d. Compared with the control group, the healing rate of the siRNA/SS-L group was reduced to 42%, suggesting the migration of 4T1 tumor cells was significantly suppressed by survivin silence ($p < 0.05$). In addition, the healing rate of the siRNA/nS-L group was higher than that of the siRNA/SS-L group, which could be explained by the slow release of siRNA in the cytoplasm due to the lack of disulfide bond in LHG2C$_{14}$. Instead, the cells treated with free siRNA showed strong migration ability, which was similar to that of the control group and was due to the minimal to negligible uptake of free siRNA by the 4T1 cells.

3.9. Cell apoptosis assay

To further evaluate the synergistic effect of co-delivering PTX and siRNA by using redox-sensitive oligopeptide liposomes, cell apoptosis induced by different formulations was determined according to the Annexin V-FITC/PI assay (Fig. 7). Similar to the cell viability results, PTX/siRNA/SS-L showed the highest total apoptotic ratio of 32.9% (the sum of the early apoptotic ratio and late apoptotic ratio), which was clearly superior to that of the siRNA/SS-L group (14.5%) and the PTX/siNC/SS-L group (13%), suggesting that synergistic apoptosis was induced by the simultaneous delivery of

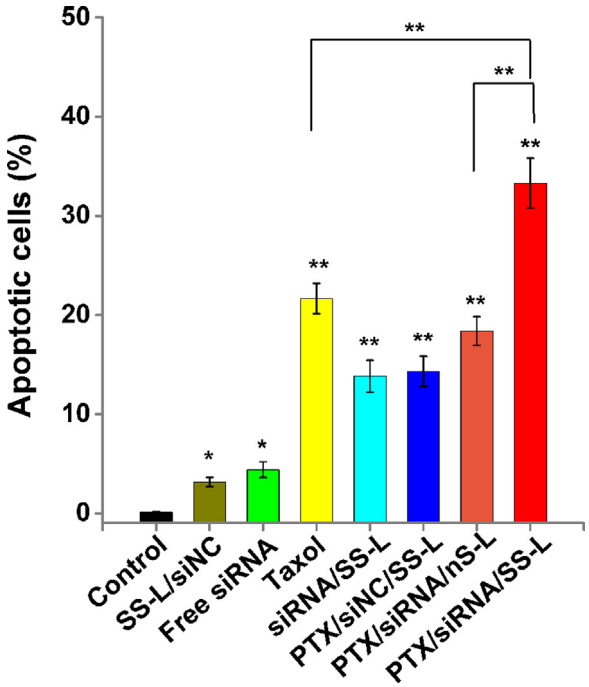

Fig. 8. Cell apoptosis rate analysis of 4T1 cells after treatment with different formulations. $^{*}p < 0.05$, $^{**}p < 0.01$.

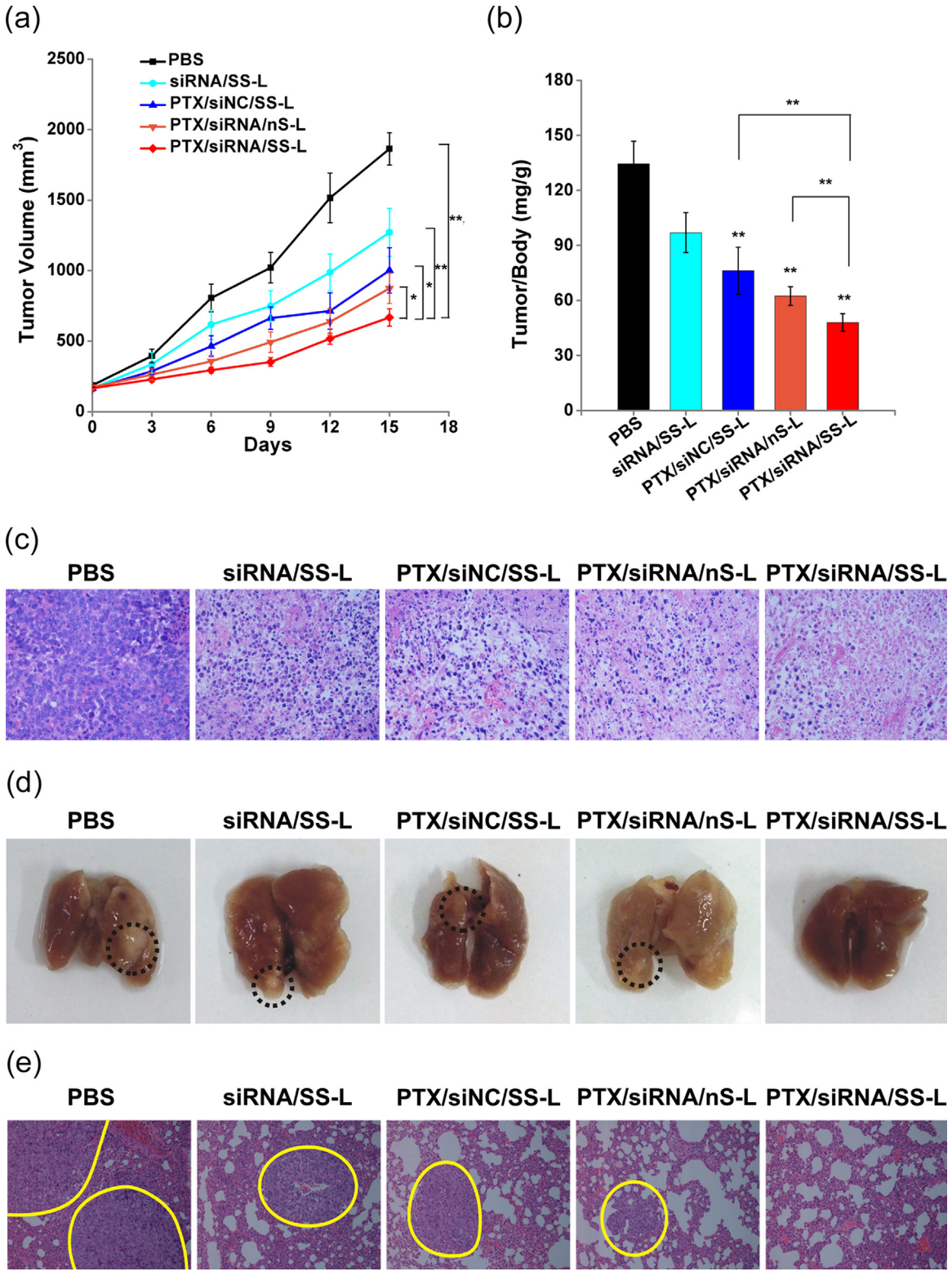

Fig. 9. *In vivo* antitumor efficacy of PTX/siRNA/SS-L in xenograft 4T1 tumor-bearing mice. (a) Tumor volume of the 4T1 tumor-bearing mice after administration of different formulations. $^{*}p < 0.05$, $^{**}p < 0.01$. (b) Weight ratio of tumor to body of the mice after treating with different formulations. $^{**}p < 0.01$. (c) The histological sections of the tumor tissues. (d) The representative images of lung tissues. (e) The histological sections of lung tissues stained with H & E after administration of different formulations. Yellow circles represent the cancer nests in lung tissues, whereas black circles represent the metastatic nodules in lung tissues. (For interpretation of the references to colour in this figure legend, the reader is referred to the web version of this article.)

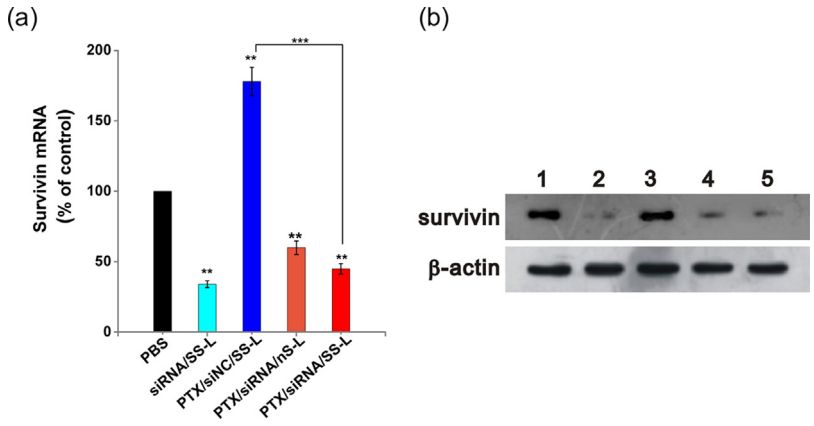

Fig. 10. (a) Survivin mRNA expression in tumor tissues after treatment with different formulations. $^{**}p < 0.01$, $^{***}p < 0.001$. (b) Protein expression in tumor tissues after treatment with different formulations. 1: PBS, 2: siRNA/SS-L, 3: PTX/siNC/SS-L, 4: PTX/siRNA/nS-L, 5: PTX/siRNA/SS-L.

anti-survivin siRNA and PTX. Moreover, the total apoptotic rate of PTX/siRNA/SS-L was higher than that of PTX/siRNA/nS-L, which indicated that the rapid release of the two drugs in the cytoplasm was conducive to enhancing their pro-apoptosis capability (Fig. 8). Taxol® also induced a higher level of apoptosis, which was similar to the results of cell activity and probably due to the toxic effect of Cremophor EL.

3.10. In vivo pharmacodynamics study

In vivo antitumor experiments were conducted on xenograft 4T1 tumor-bearing mice to evaluate the advantages of PTX/siRNA/SS-L in breast cancer therapy. As shown in Fig. 9a, the PTX/siRNA/SS-L group displayed the slowest tumor growth speed among all treatment groups, and the tumor size decreased to 35% of that of the PBS group ($p < 0.01$) and 60% of that of the PTX/siNC/SS-L group ($p < 0.01$), thereby proving that the growth of breast tumors was significantly inhibited by the treatment of PTX/siRNA/SS-L due to the synergistic anti-tumor efficacy of anti-survivin siRNA and PTX, which was also supported by the result that the weight ratio of tumor to mouse body of the PBS group was 2.8-fold higher than that of the PTX/siRNA/SS-L group ($p < 0.01$) (Fig. 9b). Meanwhile, the pathological sections (Fig. 9c) of tumor tissues of the PTX/siRNA/SS-L group showed that the number of the tumor nuclei that stained dark blue was significantly less than that of the other groups, indicating that PTX/siRNA/SS-L induced the maximum level of tumor necrosis compared with other treatment groups.

Besides, the delivery of siRNA/SS-L resulted in the inhibition of migration of the 4T1 breast cancer cells *in vitro*, implying that the combination of PTX and anti-survivin siRNA may have better anti-metastatic effects. The lung tissues of the 4T1 xenograft tumor-bearing mice after treatment were excised and assessed because the lung is a general metastatic site of breast cancer (Tabariès and Siegel, 2011; Wculek and Malanchi, 2015). As shown in Fig. 9d, white tumor nodules could be seen on the surface of the lungs in the PBS control group, suggesting the occurrence of lung metastasis of breast cancer. However, no white tumor nodules appeared on the surface of the lungs in the PTX/siRNA/SS-L group. The pathological sections of lung tissues were also observed to further investigate whether PTX/siRNA/SS-L can effectively inhibit lung metastasis of breast cancer. As shown in Fig. 9e, two huge cancer nests (circled regions) were found in the pathological sections of lung tissues in the PBS group but barely seen in the pathological sections of lung tissues in the PTX/siRNA/SS-L group, indicating the apparent prevention of lung metastasis after treatment with PTX/siRNA/SS-L. In sum, PTX/siRNA/SS-L not only suppressed tumor growth, but also prevented metastasis of breast cancer cells to the lungs, thereby indicating that PTX/siRNA/SS-L is a valuable drug system for breast cancer therapy.

The survivin expression *in vivo* was assayed by RT-PCR and western blot analysis. In accordance with the results of survivin gene expression *in vitro*, the PTX/siRNA/SS-L group showed the strongest gene silencing efficiency with 55% downregulation in tumor tissues (Fig. 10a). Additionally, the PTX/siRNA/SS-L group also exhibited more extensive suppression of the expression of survivin protein in tumor tissues compared to that of the PBS group (Fig. 10b). The observed reduction in survivin levels *in vivo* proved that PTX/siRNA/SS-L successfully delivered anti-survivin siRNA to its target, suggesting that the redox-sensitive liposome-based nanocarrier is an effective gene vector for cancer therapy. Furthermore, the downregulation of survivin may be the major reason for the improvement in anticancer efficiency.

To evaluate the toxicity of PTX/siRNA/SS-L *in vivo*, we assessed the body weight, organ index, and the pathological slices of other organs (heart, spleen, kidney, and liver) of the mice after treatment with different formulations (Fig. 11a–c). All formulations apparently did not lead to a reduction in body weight, and no statistical difference in organ index to that of the PBS group was detected. Similarly, there was no clear distinction in the pathological slices of corresponding organs. Based on these results, we concluded that the combination of anti-survivin siRNA and PTX produced fewer adverse effects and less damage to normal organs, and the redox-sensitive oligopeptide liposomes as a co-delivery nanocarrier were safe *in vivo* at the tested dosage.

4. Conclusion

In summary, to overcome PTX resistance and enhance antitumor efficacy in breast cancer, we have developed the redox-sensitive oligopeptide liposomes for simultaneously delivering PTX and anti-survivin siRNA. We showed that this nanocarrier could successfully deliver two drugs into breast cancer cells, efficiently escape endolysosomes, and rapidly collapse to release drugs into the cytoplasm. The released anti-survivin siRNA remarkably blocked the PTX-induced expression of survivin, thereby decreasing cell proliferation and wound healing rate, as well as increasing cell apoptosis. Importantly, PTX/siRNA/SS-L not only exhibited the most powerful effect on suppressing tumor growth, but also significantly restricted pulmonary metastasis. Therefore, the combination of PTX and anti-survivin siRNA is a

promising strategy to synergistically inhibit breast tumor growth and metastasis, and the redox-sensitive oligopeptide liposomes may be a potent drug nanocarrier for combined cancer therapy.

5. Conflicts of interest

None.

Acknowledgments

The National Natural Science Foundation of China (81273468, 81473153, 81503003, and 81503006), National Basic Research Program of China (2015CB755500), Natural Science Foundation of Jiangsu Province of China (BK20140672, BK20150698), Fundamental Research Funds for the Central Universities of China (2632017ZD06, 2015PY014), 111 Projects from the Ministry of Education of China and the State Administration of Foreign Expert Affairs of China (No. 111-2-07), and National Training Program of Innovation and Entrepreneurship for Undergraduates (201610316098) supported this study. We thank LetPub (www.letpub.com) for its linguistic assistance during the preparation of this manuscript.

Appendix A. Supplementary data

Supplementary data associated with this article can be found, in the online version, at **http://dx.doi.org/10.1016/j.ijpharm.2017.06.071**.

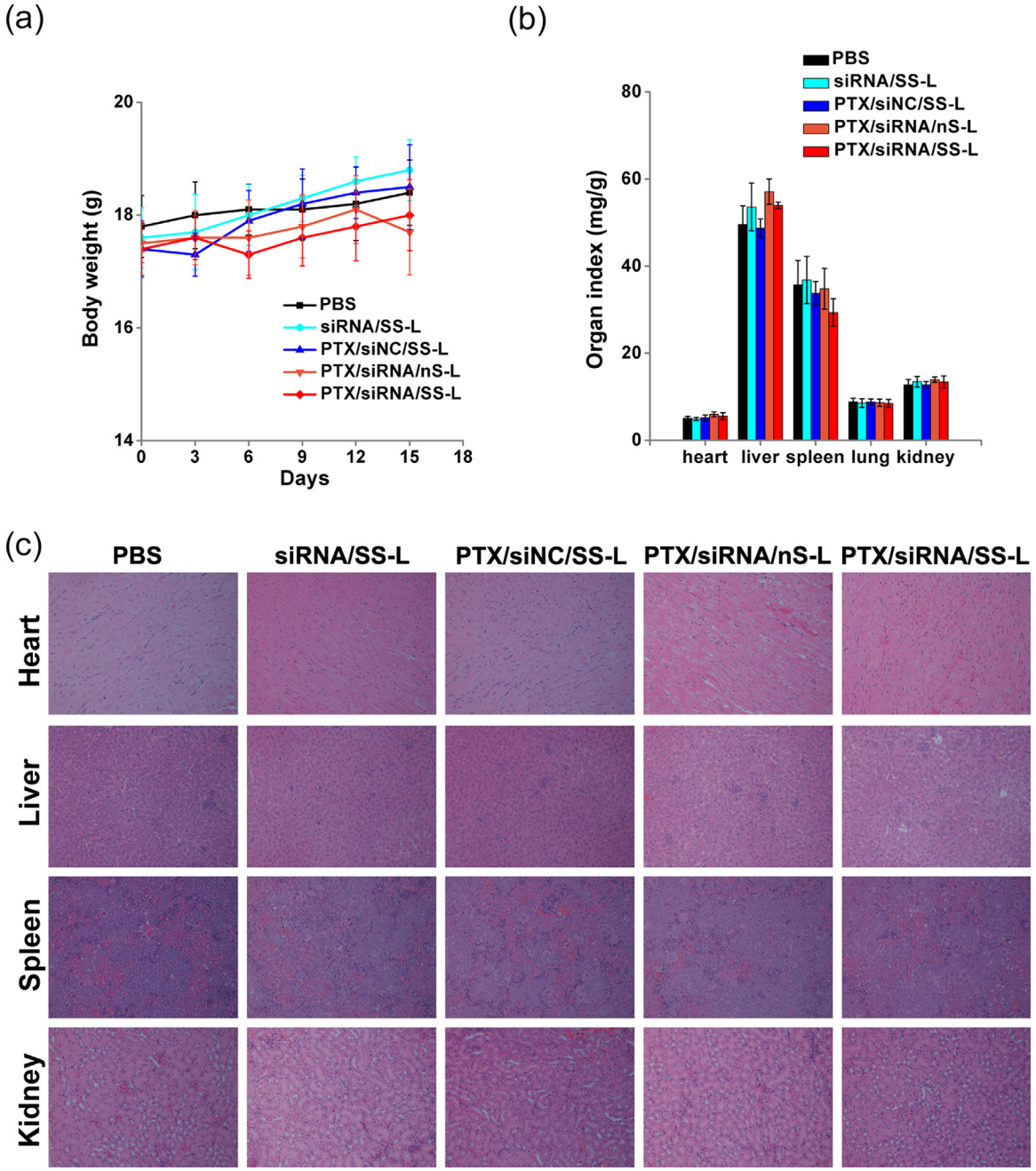

Fig. 11. (a) Body weight of mice after treatment with different formulations. (b) Organ index including heart, liver, spleen, lung, and kidney after administration of different formulations. (c) The histological characteristics of various organs (heart, liver, spleen, and kidney) after treatment with PBS, siRNA/SS-L, PTX/siNC/SS-L, PTX/siRNA/SS-L and PTX/siRNA/nS-L, respectively.

References

Chu, X.Y., Chen, L.B., Wang, J.H., Su, Q.S., Yang, J.R., Lin, Y., Xue, L.J., Liu, X.B., Mo, X.B., 2012. Overexpression of survivin is correlated with increased invasion and metastasis of colorectal cancer. J. Surg. Oncol. 105, 520–528.

Coumar, M.S., Tsai, F.Y., Kanwar, J.R., Sarvagalla, S., Cheung, C.H., 2013. Treat cancers by targeting survivin: just a dream or future reality? Cancer Treat. Rev. 39, 802–811.

Ding, Y., Zhou, Y.Y., Chen, H., Geng, D.D., Wu, D.Y., Hong, J., Shen, W.B., Hang, T.J., Zhang, C., 2013. The performance of thiol-terminated PEG-paclitaxel-conjugated gold nanoparticles. Biomaterials 34, 10217–10227.

Fröhlich, E., 2012. The role of surface charge in celular uptake and cytotoxicity of medical nanoparticles. Int. J. Nanomed. 7, 5577–5591.

Gandhi, N.S., Tekade, R.K., Chougule, M.B., 2014. Nanocarrier mediated delivery of siRNA/miRNA in combination with chemotherapeutic agents for cancer therapy: current progress and advances. J. Control. Release 194, 238–256.

Ho, T.F., Peng, Y.T., Chuang, S.M., Lin, S.C., Feng, B.L., Lu, C.H., Yu, W.J., Chang, J.S., Chang, C.C., 2009. Prodigiosin down-regulates survivin to facilitate paclitaxel sensitization in human breast carcinoma cell lines. Toxicol. Appl. Pharm. 235, 253–260.

Holohan, C., Van Schaeybroeck, S., Longley, D.B., Johnston, P.G., 2013. Cancer drug resistance: an evolving paradigm. Nat. Rev. Cancer 13, 714–726.

Hu, Q., Li, W., Hua, X., Hua, Q., Shen, J., Jin, X., Zhou, J., Tang, G., Chu, P.K., 2012. Synergistic treatment of ovarian cancer by co-delivery of survivin shRNA and paclitaxel via supramolecular micellar assembly. Biomaterials 33, 6580–6591.

Jain, V., Swarnakar, N.K., Mishra, P.R., Verma, A., Kaul, A., Mishra, A.K., Narendra, K., Jain, N.K., 2012. Paclitaxel loaded PEGylated gleceryl monooleate based nanoparticulate carriers in chemotherapy. Biomaterials 33, 7206–7220.

Jha, K., Shukla, M., Pandey, M., 2012. Survivin expression and targeting in breast cancer. Surg. Oncol. 21, 125–131.

Jordan, M.A., Wilson, L., 2004. Microtubules as a target for anticancer drugs. Nat. Rev. Cancer 4, 253–265.

Khan, S., Bennit, H.F., Turay, D., Perez, M., Mirshahidi, S., Yuan, Y., Wall, N.R., 2014. Early diagnostic value of survivin and its alternative splice variants in breast cancer. BMC Cancer 14, 176.

Kobayashi, H., Watanabe, R., Choyke, P.L., 2014. Improving conventional enhanced permeability and retention (EPR) effects: what is the appropriate target? Theranostics 4, 81–89.

Lee, E., Oh, C., Kim, I.S., Kwon, I.C., Kim, S., 2015. Co-delivery of chemosensitizing siRNA and an anticancer agent via multiple monocomplexation-induced hydrophobic association. J. Control. Release 210, 105–114.

Li, J., Huo, M., Wang, J., Zhou, J., Mohammad, J.M., Zhang, Y., Zhu, Q., Waddad, A.Y., Zhang, Q., 2012. Redox-sensitive micelles self-assembled from amphiphilic hyaluronic acid-deoxycholic acid conjugates for targeted intracellular delivery of paclitaxel. Biomaterials 33, 2310–2320.

Li, J., Liu, J., Guo, N., Zhang, X., 2016. Reversal of multidrug resistance in breast cancer MCF-7/ADR cells by h-R3-siMDR1-PAMAM complexes. Int. J. Pharm. 511, 436–445.

Ling, X., Bernacki, R.J., Brattain, M.G., Li, F., 2004. Induction of survivin expression by taxol (paclitaxel) is an early event, which is independent of taxol-mediated G2/M arrest. J. Biol. Chem. 279, 15196–15203.

Marino, N., Woditschka, S., Reed, L.T., Nakayama, J., Mayer, M., Wetzel, M., Steeg, P.S., 2013. Breast cancer metastasis: issues for the personalization of its prevention and treatment. Am. J. Pathol. 183, 1084–1095.

Midoux, P., Pichon, C., Yaouanc, J.J., Jaffrès, P.A., 2009. Chemical vectors for gene delivery: a current review on polymers, peptides and lipids containing histidine or imidazole as nucleic acids carriers. Br. J. Pharmacol. 157, 166–178.

Mo, R., Jin, X., Li, N., Ju, C.Y., Sun, M.J., Zhang, C., Ping, Q.N., 2011. The mechanism of enhancement on oral absorption of paclitaxel by N-octyl-O-sulfate chitosan micelles. Biomaterials 32, 4609–4620.

Mo, R., Sun, Q., Xue, J., Li, N., Li, W., Zhang, C., Ping, Q., 2012. Multistage pH-responsive liposomes for mitochondrial-targeted anticancer drug delivery. Adv. Mater. 24, 3659–3665.

Montazeri Aliabadi, H., Landry, B., Mahdipoor, P., Uludağ, H., 2011. Induction of apoptosis by survivin silencing through siRNA delivery in a human breast cancer cell line. Mol. Pharm. 8, 1821–1830.

Murray, S., Briasoulis, E., Linardou, H., Bafaloukos, D., Papadimitriou, C., 2012. Taxane resistance in breast cancer: mechanisms, predictivebiomarkers and circumvention strategies. Cancer Treat. Rev. 38, 890–903.

Parvani, J.G., Davuluri, G., Wendt, M.K., Espinosa, C., Tian, M., Danielpour, D., Sossey-Alaoui, K., Schiemann, W.P., 2015. Deptor enhances triple-negative breast cancer metastasis and chemoresistance through coupling to survivin expression. Neoplasia 17, 317–328.

Promkan, M., Liu, G., Patmasiriwat, P., Chakrabarty, S., 2011. BRCA1 suppresses the expression of survivin and promotes sensitivity to paclitaxel through the calcium sensing receptor (CaSR) in human breast cancer cells. Cell Calcium 49, 79–88.

Qu, M.H., Zeng, R.F., Fang, S., Dai, Q.S., Li, H.P., Long, J.T., 2014. Liposome-based co-delivery of siRNA and docetaxel for the synergistic treatment of lung cancer. Int. J. Pharm. 474, 112–122.

Salzano, G., Riehle, R., Navarro, G., Perche, F., De Rosa, G., Torchilin, V.P., 2014. Polymeric micelles containing reversibly phospholipid-modified anti-survivin siRNA: a promising strategy to overcome drug resistance in cancer. Cancer Lett. 343, 224–231.

Salzano, G., Navarro, G., Trivedi, M.S., De Rosa, G., Torchilin, V.P., 2015. Multifunctional polymeric micelles co-loaded with anti-survivin siRNA and paclitaxel overcome drug resistance in an animal model of ovarian cancer. Mol. Cancer Ther. 14, 1075–1084.

Shigeta, K., Kawakami, S., Higuchi, Y., Okuda, T., Yagi, H., Yamashita, F., Hashida, M., 2007. Novel histidine-conjugated galactosylated cationic liposomes for efficient hepatocyte-selective gene transfer in human hepatoma HepG2 cells. J. Control. Release 118, 262–270.

Siegel, R., Ma, J., Zou, Z., Jemal, A., 2014. Cancer statistics, 2014. CA Cancer J. Clin. 64, 9–29.

Singh, N., Krishnakumar, S., Kanwar, R.K., Cheung, C.H., Kanwar, J.R., 2015. Clinical aspects for survivin: a crucial molecule for targeting drug-resistant cancers. Drug Discov. Today 20, 578–587.

Sun, T.M., Du, J.Z., Yao, Y.D., Mao, C.Q., Dou, S., Huang, S.Y., Zhang, P.Z., Leong, K.W., Song, E.W., Wang, J., 2011. Simultaneous delivery of siRNA and paclitaxel via a two-in-one micelleplex promotes synergistic tumor suppression. ACS Nano 5, 1483–1494.

Sun, Q., Kang, Z., Xue, L., Shang, Y., Su, Z., Ping, Q., Mo, R., Zhang, C., 2015. A collaborative assembly strategy for tumor-targeted siRNA delivery. J. Am. Chem. Soc. 137, 6000–6010.

Tabariès, S., Siegel, P.M., 2011. Breast cancer liver metastasis. In: Brodt, P. (Ed.), Liver Metastasis: Biology and Clinical Management. Springer, Netherlands, pp. 273–303.

Verma, K., Ramanathan, K., 2015. Investigation of paclitaxel resistant R306C mutation in β-tubulin—a computational approach. J. Cell. Biochem. 116, 1318–1324.

Wang, T., Gantier, M.P., Xiang, D., Bean, A.G., Bruce, M., Zhou, S.F., Khasraw, M., Ward, A., Wang, L., Wei, M.Q., Alshamaileh, H., Chen, L., She, X., Lin, J., Kong, L., Shigdar, S., Duan, W., 2015. EpCAM aptamer-mediated survivin silencing sensitized cancer stem cells to doxorubicin in a breast cancer model. Theranostics 5, 1456–1472.

Wculek, S.K., Malanchi, I., 2015. Neutrophils support lung colonization of metastasis-initiating breast cancer cells. Nature 528, 413–417.

Yang, Z.Z., Li, J.Q., Wang, Z.Z., Dong, D.W., Qi, X.R., 2014. Tumor-targeting dual peptides-modified cationic liposomes for delivery of siRNA and docetaxel to gliomas. Biomaterials 35, 5226–5239.